Intraseasonal oscillation of tropical convergence zones: Theory and prediction

Ravi S. Nanjundiah[1,*] and T. N. Krishnamurti[2]

[1]Centre for Atmospheric and Oceanic Sciences, Indian Institute of Science, Bangalore 560 012, India
[2]Department of Meteorology, Florida State University, Tallahasse, FL, 32306-4520, USA

The intraseasonal oscillation of Tropical Convergence Zones (TCZ) over the Indo-Pacific region has been studied. Both meridional and zonal propagating modes with timescales of about 40 days are prominent over the Indian and West Pacific regions. The mechanisms governing both these modes are reviewed. It is found that ocean–atmospheric interaction plays an important role in modulating these modes. The role of oceans is further highlighted in a series of seasonal forecasts using a coupled ocean–atmosphere model. It is found that forecasts of intraseasonal oscillations show significant improvement upon assimilation of sub-surface ocean data from the ARGO (a global programme to observe sub-surface profiles in the oceans) array of floats.

Keywords: Intraseasonal variation, prediction, Tropical convergence zones.

THE MJO/ISO (Madden–Julian Oscillation/Intraseasonal Oscillation) simulations and forecasts have been an area of great scientific interest in recent years. At present, diversity of opinion exists on the modelling of this phenomenon. One needs to understand the central issues that govern the structure, motion and maintenance of this phenomenon. Some authors emphasize the pivotal role of cumulus convection for the maintenance of the MJO/ISO[1–4]. Randall *et al.*[2] emphasize the need for a cloud resolving non-hydrostatic microphysical model for its simulation. Nakazawa[5] observed that an envelope moving east on the time scale of 20 to 60 days, carries within it cloud lines that propagate eastward at a phase speed of roughly 5 to 7 degrees longitude per day. These two scales seem to move in unison and closely coupled. There are other studies that seem to provide simulations of the MJO without recourse to the explicit cloud modelling. Zhang and Mu[3] showed that refinement of cumulus parameterization is central for the modelling of this phenomenon. They found that a refinement of the Zhang-McFarlane[6] cumulus parameterization scheme was necessary for the simulation. He utilized an NCAR coupled model: the CCM3. Two separate studies[7,8] emphasized the need for uncoupled and coupled models for the modelling of the MJO. Wave–CISK (conditional instability of the second kind) was proposed[4] following the work of Lindzen[9] as a source of excitation for the globally traversing MJO waves. This called for a modulation of equatorial Kelvin waves from the effects of wave-induced convection as contrasted from ordinary CISK that calls for Ekman convergence for the drive of convection.

Poleward propagation of rainbands starting from near the equator and culminating in the northern trough zone is a unique feature of Intertropical Convergence Zones (ITCZ) over the Indo-Pacific region[10].

In this article we look at mechanisms governing MJO/ISO (both zonally and meridionally migrating systems). We propose that the oceans have a major role on these timescales of several months. We feel that coupled assimilation with a good coverage of global data in the atmosphere and in the ocean is important. Towards this end we have exploited the ECMWF database, the best estimates of precipitation for the atmospheric part of the data assimilation and the Reynolds SSTs (sea surface temperatures) and the global ARGO database for the oceans.

Mechanisms governing ISO

We first discuss mechanisms governing zonally moving ISO over the equatorial region and this is followed by a discussion of mechanisms governing the poleward moving ISO which are prominent during the northern summer (June–September) season over the Indo-Pacific region.

Zonally propagating ISO

Various theories have been proposed to explain the eastward movement of ISO. Majority of the mechanisms invoke the interaction of heating and movement of waves. The theories can be broadly classified as follows: i) Wave–CISK mechanism, ii) WISHE mechanism, iii) Charge–discharge theory, iv) Wave–wave interaction in spectral space.

Many excellent reviews[11,12] have discussed these mechanisms (i–iii). We therefore discuss them briefly here. The mechanisms (i–iii) suffer from the shortcoming that many assumptions have to be made to select the right scale (i.e. the planetary scale). The wave–wave interaction mechanism has the advantage that the combination

*For correspondence. (e-mail: ravi@caos.iisc.ernet.in)

of waves selects the correct wave number on the intraseasonal scale for amplification.

Wave–CISK mechanism. This mechanism is based on the theory for development of tropical cyclones[13,14]. CISK explains the co-operative development mechanism of larger scale tropical cyclones due to heating at cumulus scales embedded in the tropical cyclones. The frictional convergence within the boundary layer supplies moisture to support cumulus convection and the heating due to cumulus convection intensifies the tropical cyclone. Attempts have been made to extend this theory to equatorial ISO[15] by proposing a feedback mechanism between cumulus convection and equatorial waves. In contrast to conventional CISK, in which boundary layers processes such as drag and fluxes could play a prominent role, the interaction between equatorial waves and cumulus convection was largely inviscid and hence was termed as wave–CISK[9]. A further modification of this was the mobile wave–CISK mechanism[4]. According to this theory, eastward propagation of MJO arises due to an interaction between modes of convection and Kelvin waves, i.e. instead of Ekman pumping at the top of the boundary layer, waves induced convergence which gave rise to cumulus convection. Lau and Peng[4] find that upon making the heating nonlinear (i.e. positive only) Kelvin waves are amplified. The time period for the eastward MJO-like oscillation in their model is determined by the time taken by the moist Kelvin wave to go around the globe. A wave–CISK based cumulus parameterization showed that propagation of organized convection ('supercloud cluster') occurs due to the formation of new convection centres in the region of convergence of a Kelvin wave[16]. Interestingly, Lau *et al.*[16] find that while individual cloud clusters move westward, the region of convergence itself moves eastward with the characterstics of a Kelvin wave; the westward movement of cloud clusters themselves has the characterstics of a Rossby wave.

A major shortcoming of most wave–CISK models is the timescale of propagation: they exhibit faster time scales than observed. The prescription of vertical profile of heating also appears to be a matter of dispute. Some studies show that incorporation of heating maxima in the lower troposphere gives realistic timescales[17]. However, Cho and Pendelbury[18] suggest that unstable large-scale modes appear only if the heating maxima is in the upper troposphere.

Wind-induced surface heat exchange. This theory[19,20] suggests that MJO is produced as a result of instability caused by surface latent heat flux. It assumes that the tropical atmosphere is neutrally stratified. It also assumes the occurrence of mean surface easterlies. Easterlies are enhanced ahead of an eastward moving trough. This enhancement of easterlies causes increased entropy exchange from ocean to atmosphere. No cumulus convection scheme is used in their model but it is assumed that entropy transfered from the ocean to the atmosphere at the interface is redistributed throughout the atmosphere through local convection (as the atmosphere is neutrally stratified). The heating caused by entropy transfer warms the atmosphere, this warming reduces surface pressure and causes the trough to move eastward. The linear model of wind-induced surface heat exchange (WISHE) also selects shorter wavelengths for amplification but the inclusion of a time lag between large-scale forcing of convection and its response dampens the shortwaves. This hypothesis has been tested in models with mixed results. Brown and Bretherton suggest that while the phase speed is too large, presence of unsaturated downdrafts driven by evaporation destabilizes the long waves and damps the short waves. However, Lin *et al.*[22] with a more complex model found that WISHE itself was not sufficient to support MJO but it did damp out the short waves and thus encourage the growth of longer waves.

A major criticism of WISHE has been the assumption of occurrence of mean easterlies. MJO is most prominent over equatorial Indian and Pacific regions where the mean wind is westerly. Over the Eastern Pacific, WISHE explains the movement of MJO satisfactorily[23]. Maloney[24], on the contrary, reports that WISHE cannot explain the preference of their model's intraseasonal variation of convection to coincide with 850 hPa easterly anomalies. WISHE however identifies the primary source of energy for MJO, i.e. latent heat flux from the ocean surface.

Charge–discharge theory. This theory[25] links the periodicity of MJO (about 40 days) to the recharge time of the instability. Analysis of observations[26] has shown that after the passage of a MJO, mid-level moist static energy builds up with a drying of the mid-troposphere ('the charging') and this instability is consumed during the passage of a MJO ('the discharge').

Wave–wave interaction. Krishnamurti *et al.*[27] have shown that interaction of MJO timescales with that of synoptic timescales in the constant flux and boundary layers leads to a large amplification at the MJO timescales. This amplification is more prominent in the frequency domain. They show that tropical disturbances arising out of instabilities abound the synoptic timescale. The non-zero SST fluctuation on the MJO timescale (which is transmitted as intraseasonal variation of the exchange co-efficient CLH) facilitates the rapid amplification of the MJO via triad interactions (involving winds, difference in humidity and CLH, shown schematically in Figure 1). Another interesting feature noticed by them is the larger magnitude of moisture fluxes at the 850 hPa level as compared to those at the top of the constant flux layer, especially over the Indian region. Thus a small signal of SST is successively amplified via triad interactions, first over the constant flux layer and next within the PBL. Thus the amplified

MJO signal at the top of the boundary layer can be passed to the upper troposphere from cloud base (which is near the top of PBL) to cloud top through cumulus convection which have quadratic nonlinearities and can convey in-scale (MJO to MJO) information from the cloud base to cloud top. They further suggest that divergent circulations in the upper troposphere carry this signal from the regions of intense convection to other areas of the tropics.

The nature of interactions is different for sensible heat and momentum fluxes, with triads outside the synoptic role also playing a major role. Even for these fluxes, the synoptic timescales contribute significantly though they are not part of the significant triads. However, Krishnamurti *et al.*[27] suggest that it is moisture flux and neither momentum flux nor sensible heat flux that is central to their MJO theory.

The role of surface processes on MJO has been studied by Rajendran *et al.*[28]. They show that land surface processes impact the structure and frequency of propagating modes over the equator (Figure 2). When the soil moisture is kept at its mean, the annual value convection shows westward propagation over the Central Pacific and eastward propagation over Indian and West Pacific regions. In contrast, when the soil moisture is allowed to change interactively, the propagations are markedly eastward over Indian, West and Central Pacific regions. This clearly shows that surface fluxes, both remote and local, have a significant impact on MJO. It is interesting to note that Krishnamurti *et al.*[27] have found higher latent fluxes in the off-equatorial regions over the Indian longitudes. Thus, perhaps the additional timescales that variable hydrology introduces could be interacting with the surface fluxes and strengthening the eastward-propagating modes on the intraseasonal scale.

Mechanisms governing poleward propagations

Poleward propagations of rainbands are a unique feature to Indian and West Pacific latitudes[10,29]. They generate over the warm waters of the equatorial Ocean and move northward with typical speeds of about 1° per day. They culminate in the northern trough region. These oscillations are quasi-periodic with an interval of approximately 40 days between each northward-propagating event. Shanker

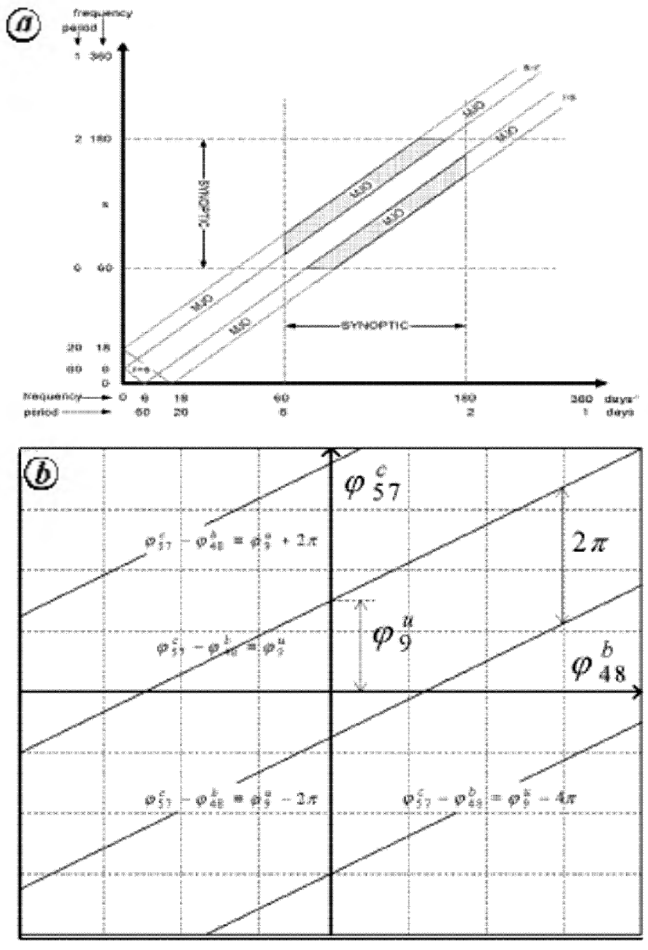

Figure 1. Schematic of interactions in the frequency domain. Synoptic timescales interact with MJO timescales to produce a triad in the MJO timescale (from Krishnamurti *et al.*[27]).

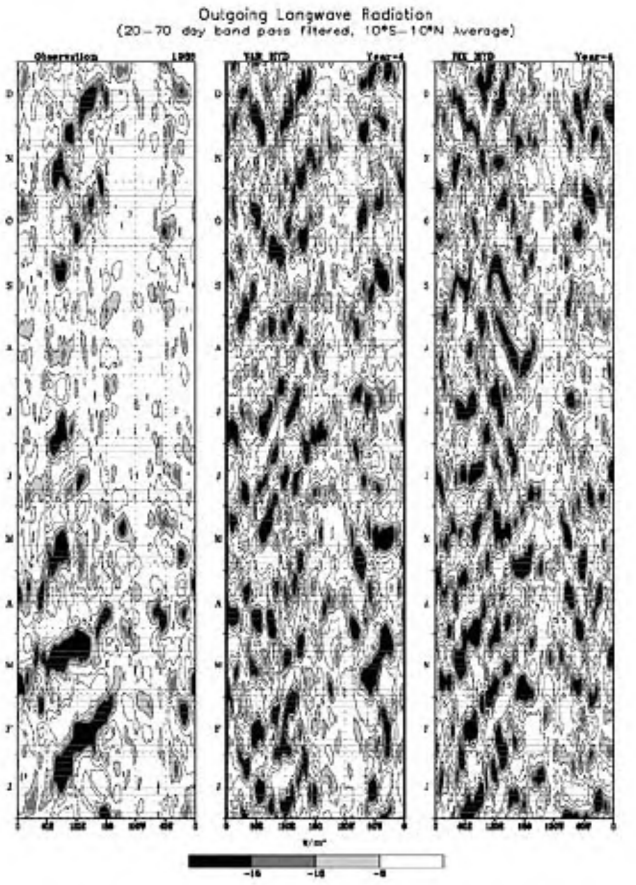

Figure 2. MJO in observations (left), (centre) in AGCM simulations with interactive hydrology and (right) in AGCM simulations with non-interactive land–surface hydrology (from Rajendran *et al.*[28]).

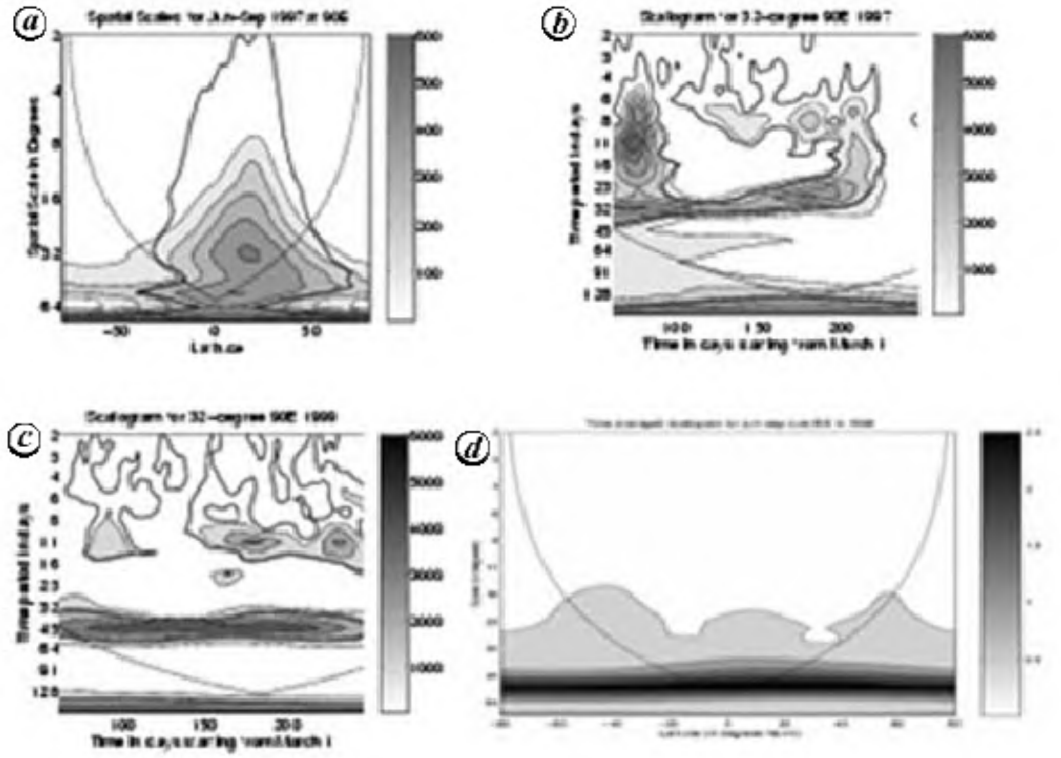

Figure 3. ***a***, The dominant spatial in daily rainfall over the Indian region during the June–September season. ***b***, Temporal scales associated with the dominant spatial scale of 32° for (***b***) 1997 and (***c***) for 1999. ***d***, Dominant spatial scale over Africa. Note the difference in spatial scales over Africa and India (from Shanker and Nanjundiah[30].)

and Nanjundiah[30] using continuous space-time wavelets have shown that the dominant spatial scale related to these latitundal variations is about 30 degrees and the associated temporal scale is about 30–40 days (Figure 3). They find that the dominant spatial scale over the Indian region remains unchanged but temporal scales show interannual variability. Over regions such as central Africa, where such propagations are not a regular feature such characteristic spatial and temporal scales are not seen (Figure 3). Many theories have been proposed to understand the poleward propagations. These can be broadly classified as those invoking dynamics and those invoking thermodynamics. Here we discuss a few of these theories. A detailed discussion of these theories can be found in refs 11, 12 and 31.

Dynamical mechanisms. Wang and Xie[7] suggest that northward propagations are a manifestation of northwestward Rossby waves from the equatorial Kelvin–Rossby wave packet over the maritime continent. These Rossby waves are also generated in West Pacific as the Kelvin–Rossby wave packet rapidly decays over the Central Pacific. This theory does not explain why the Rossby wave has a northward-propagating component.

Lau and Lau[32] had studied vorticity disturbances over Bay of Bengal, Philippine Sea and South China Sea. They proposed that these waves with a horizontal scale of about 4000 km and north-westward propagation speed of 4–5 m/s are a manifestation of unstable equatorial Rossby waves. They have also studied the northward movement in terms of rotation of the horizontal vorticity vector by equatorward gradient of vertical velocity. They assume a constant easterly vertical shear. This gives rise to a horizontal vorticity vector. About the centre of convection, if the upward velocity is higher southward, then it results in 'lifting' of the vorticity vector, resulting in a vertical component of vorticity north of the centre of convection. This vertical component of vorticity results in low level convergence north of the convection centre causing convection there and the convection centre moves northwards. The opposite effect occurs to the south of the convection centre and prevents a southward movement.

Theories based on thermodynamics. Several studies have linked poleward propagations to convection, surface heat fluxes and SST (for example, ref. 33 and others). In modelling studies, the role of interactive coupling of SST to the atmosphere for the simulation of ISOs has been highlighted by Fu and Wang[8] and Zheng *et al.*[34].

Webster[35] studied poleward propagations in a zonally symmetric model. The poleward propagations in his model began at the coastal margin and moved further north-

wards with a timescale of about 10 days. He suggested that gradient of sensible heat flux causes poleward propagations of rainbands. Since changes in sensible heat flux are relatively small over oceans, this mechanism does not explain movement of cloudbands over oceanic regions. Nanjundiah *et al.*[36], Gadgil and Srinivasan[37] and Srinivasan *et al.*[38] have also studied poleward propagations in zonally axisymmetric models. Their hypothesis explains propagations over both ocean and land. The cloudband propagates northwards from its region of genesis over the ocean due to excess of heating to the north of the axis of TCZ (axis of TCZ being identified in their model as the region of maximum ascent) relative to the region beneath the axis of TCZ or to its south. The north–south differential in total heating arises from the nature of meridional variation of the convective heating (Q_{cv}). They found that even when the vertical velocity was skewed southwards, Q_{cv} was larger northwards (Figure 4). They report that this offset between Q_{cv} and the vertical velocity profiles arises from the meridional gradient of convective instability and moisture availability (the combined effect of these two was called the intensity factor). They also found that intensity factor increases with increasing surface temperature and attains its maximum value in the trough zone. The poleward propagation occurs due to poleward gradient of this factor. In the absence of a gradient in this factor, poleward propagations cease in their models. Over land, both moisture availability and convective instability can modulate the intensity factor, while ocean with moisture availability not being a constraint only convective instability plays a role in modulating poleward propagations. It is interesting to note that the dynamical theory of Lau and Lau[32] and that of Nanjundiah *et al.*[36] is similar in one respect: the vertical ascent could be higher to the south of the cloudband but the band moves northwards due to convergence occurring north of the band, in one case it is the poleward gradient of the convective instability factor and in the other it is the lifting of horizontal vorticity vector.

Rajendran *et al.*[39] examined poleward propagations in an AGCM. They found that their model simulated better ISO upon using the moist convective adjustment rather than the mass flux Hack scheme (Figure 5). Poleward propagations were more prominent upon using the convective adjustment scheme. They examined the meridional variation of moist static energy in the lower troposphere (which governs the moist vertical static stability) in NCEP/NCAR reanalysis and in their simulations with Hack parameterization scheme and the Moist Convective Adjustment (MCA) scheme. They found that NCEP and MCA showed favourable gradient between 5°N and 25°N. However, in the Hack simulation the moist static energy did not increase beyond 10°N and thus resulted in less prominent poleward propagations. They also showed that zonal ISO were also better simulated upon prescription of the MCA scheme.

Predictability and prediction of ISO

Waliser *et al.*[40] have discussed the extent of predictability in a GCM. They suggest that strong MJO events could be predictable up to four weeks while the predictability for weaker MJOs is much less.

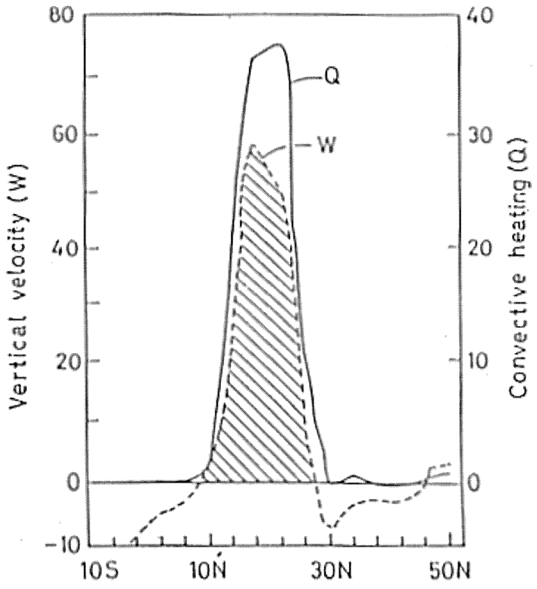

Figure 4. The asymmetry between region of maximum ascent (the axis of TCZ) and region of maximum heating (from Nanjundiah *et al.*[36]).

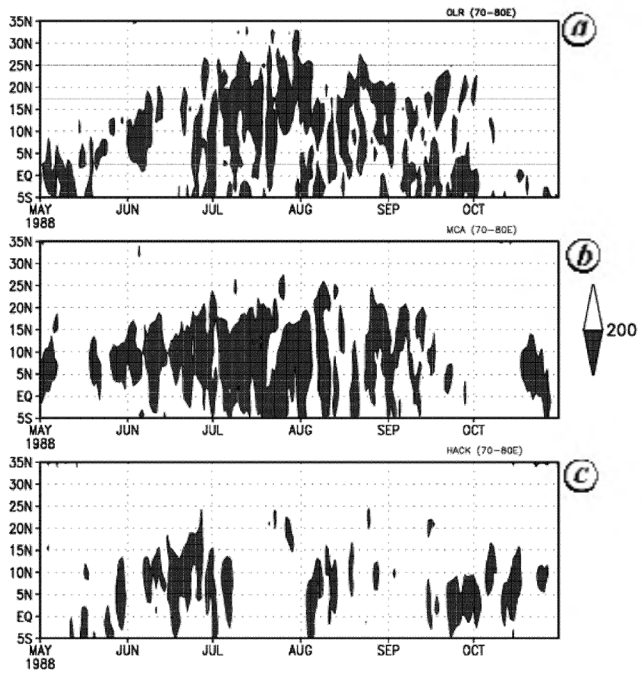

Figure 5. Poleward propagations of OLR in (*a*) observations, (*b*) using moist convective adjustment scheme and (*c*) using Hack scheme (from Rajendran *et al.*[39]).

Waliser *et al.*[41] discuss the prediction of MJOs using both dynamical and statistical methods under the Experimental MJO Prediction Programme (EMPP). In this project, six statistical-empirical models and three coupled models are used. The statistical models vary from multiple regression linear models to empirical wave-propagation models. Their major conclusion is that considerable research is required for predictions on the intraseasonal scales to reach the levels of skills currently available in short-term forecasts. They report that on an average the correlation co-efficient for tropical velocity potential is about 0.3. However, there are swings in the co-efficients which are unrealistic and unrelated to MJO. These swings are more prominent in statistical models. For GCMs the skills are even lower at about 0.1 over the warm pool region.

A detailed discussion on empirical methods for prediction of monsoon ISO can be found in Xavier and Goswami[42] (this issue).

Role of oceans in monsoon ISO

This section is a short summary a forthcoming paper by Krishnamurti and his colleagues[43]. The current availability of a vast satellite-based real time data components (as many as 69 millions distinct observations per day) and the advent of the global ARGO floats (as many as 2700 oceanic measurements) provided a unique opportunity to explore the coupled assimilation of this data stream and its impact on global seasonal climate forecasts. They examine the meridional passage of the monsoon intraseasonal oscillations in the subsurface oceans.

Figure 7 illustrates a current distribution of the ARGO floats over the global oceans. This provides ocean temperature; salinity and ocean currents to the depth of 2 km. Data at every 10 days are transmitted and received from satellites, making this one of the most impressive oceanic data components for real time.

Krishnamurti *et al.*[43] used the Florida State University (FSU) global spectral model (GSM) coupled with a modified version of HOPE ocean model to study the impact of ARGO temperature profiles on the forecasts of ISO over the Indian subcontinent. The atmospheric model had a triangular resolution at 63 waves (T63) that corresponds to roughly 1.875 degrees near the Equator. It had 14 vertical sigma levels. The ocean model had constant horizontal resolution of 5 degrees along longitude and a varying 0.5 to 5.0 degree in latitude, higher resolution being near the Equator. The ocean model had 17 vertical levels. Ten of these levels appeared in the upper 300 m of the ocean to resolve the upper ocean dynamics with high precision.

The model spin-up and coupled assimilation carried out in this work[43] contain the following two components:

Ocean assimilation phase

The first component of data assimilation is on ocean spin up that is carried out for a 10-year period, 1978 through 1987. Krishnamurti *et al.*[43] used a Newtonian relaxation method to nudge the SST to the Reynolds SST. The other external forcing for the ocean model are imposed wind stresses where the monthly mean winds for the period 1978–1987 are used to spin up the ocean. The details of this procedure are discussed in refs 44 and 45.

Coupled assimilation

This is a daily assimilation of the ocean and the atmosphere using the ECMWF analysis for the atmosphere and the observed Reynolds SSTs for the ocean. In addition, this includes an assimilation of the ARGO profiles of

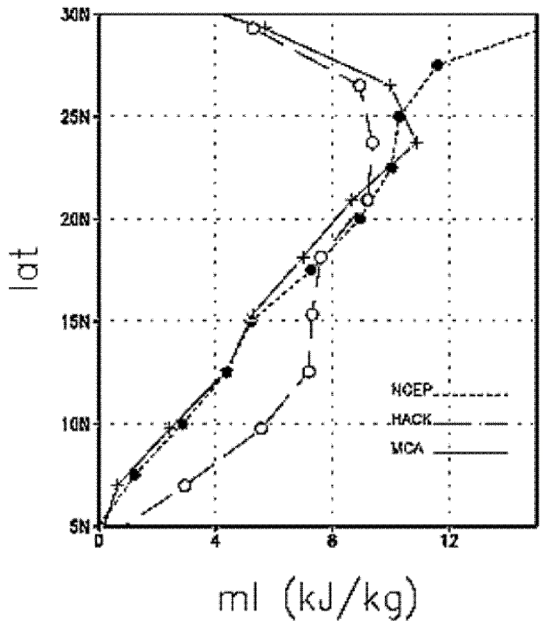

Figure 6. Meridional variation of moist static energy in the lower troposphere in NCEP–NCAR re-analysis, simulations with Hack scheme and simulations with the MCA scheme (from Rajendran *et al.*[39]).

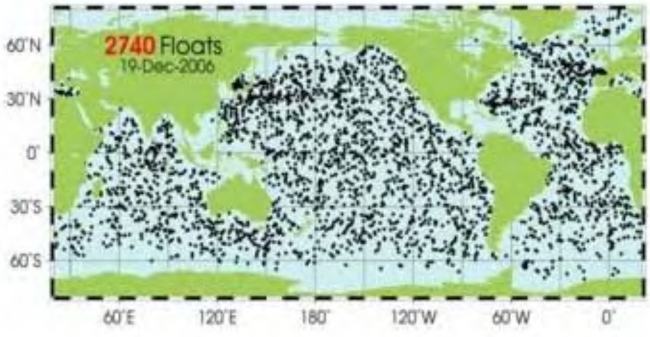

Figure 7. Positions of the ARGO floats.

ocean temperatures. An additional feature in this coupled assimilation is the rain rate initialization. This is described in some detail by Krishnamurti and his colleagues[46,47].

Krishnamurti *et al.*[43] next examine the prediction of the meridionally propagating ISO wave across the Indian subcontinent. Observational studies[10,29,48] addressed respectively the meridional passage of the ISO wave across the Indian subcontinent for clouds, winds and precipitation. Basically this wave has roughly a timescale of 20 to 60 days with a northward-propagating speed of 1° latitude/day and has zonal and meridional wavelengths of roughly 3000 km. In the wind field clockwise and counterclockwise gyres of circulation seem to form near 5°S (over the southern equatorial trough) and propagate northward. They noted that seasonal forecasts, using multimodels, carry this feature in the atmosphere and the subsurface of the coupled atmosphere–ocean model. The results from the ensemble mean of the four models were compared with the analysis fields. Specifically they compared multimodel forecasts to illustrate the differences from the inclusion versus exclusion of the ARGO data sets.

The meridional propagation of an ISO wave in the Indian Ocean region (integrated between 90° and 95°E) is shown in Figure 8. It shows the ISO timescale propagation (latitude–time diagrams) at the ocean surface and the subsurface temperature fields at 0, 20 and 40 m depths. In this figure the meridional passage of ISO wave at the ocean surface and at the 20 and 40 m depths is clearly evident. The amplitude of this wave is only almost one tenth of a degree centigrade. The rate of meridional propagation is around 1° latitude per day. The results at the surface and subsurface levels are coherent. The small amplitude is not a matter of concern since the ISO/MJO wave carry amplitudes which is only 10% of the total field in the atmosphere.

The corresponding atmospheric component of the ISO wave can be located at the 850 hPa level. These show up prominently in the zonal wind anomalies of this time scale. Figure 9 illustrates the corresponding latitude–time diagram at the 850 hPa level for the zonal wind on this timescale. Figure 9 *a* shows this field based on ECMWF analysis. Figures 9 *b* and *c* show the seasonal forecasts from the control and the ARGO runs respectively. It is clear that a close match to the observed meridional phase/amplitude propagation is predicted by the coupled models when the ARGO data were assimilated. The rate of meridional propagation is around 1° latitude per day, the zonal wind anomalies on this modelling carry amplitude of roughly 3–4 m s^{-1}. Overall this shows a robust modelling of the ISO wave when the ARGO temperature profile is assimilated. Krishnamurti *et al.*[43] have also noted that meridional propagation of cold anomalies at the ocean surface and at the subsurface coincide with the meridional passage of westerly wind anomalies at the 850 hPa level and vice versa.

Another modelling aspect of the ISO/MJO includes forecasts of a few cycles for this feature. This is described in the three-part paper by Krishnamurti and his colleagues[49–51]. In these studies the premise was that an initial state that excludes the high frequency modes can carry the low frequency, i.e. the ISO/MJO scale for a few cycles without any large contamination. It has been shown

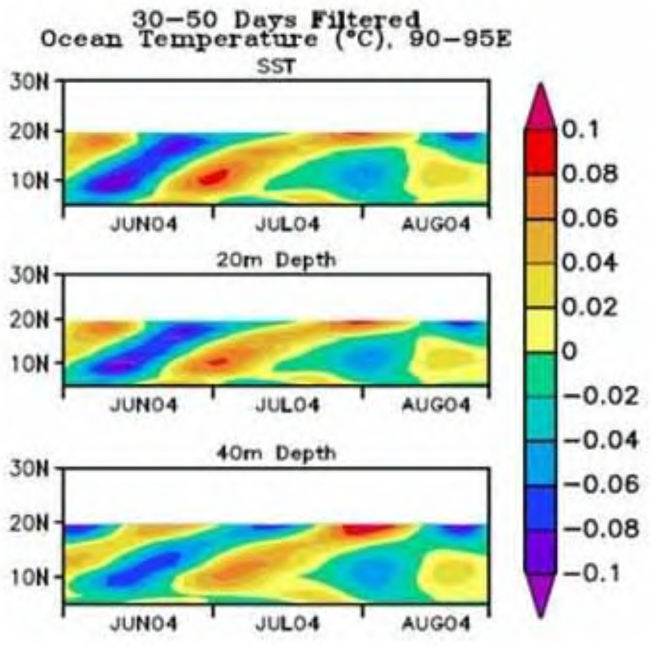

Figure 8. Meridional migration of intraseasonal oscillation of ocean temperature at 30–50 days timescale at different depths from ARGO forecasts of the model over the Bay of Bengal.

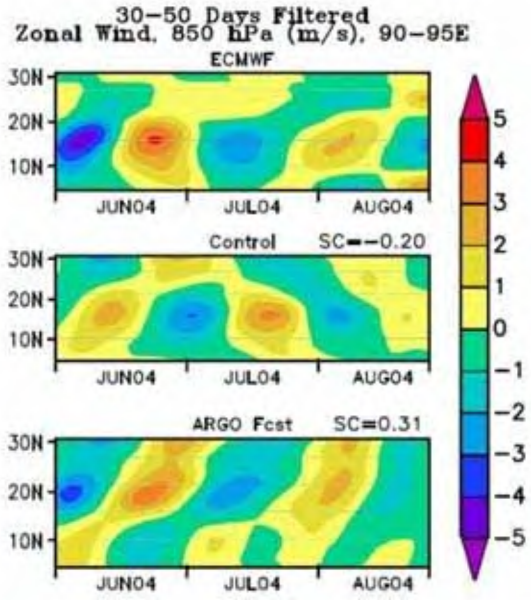

Figure 9. Meridional migration of zonal wind at 850 hPa level over the Bay of Bengal from ECMWF analysis, and control and ARGO forecasts of the model.

from observational scale interaction studies[52] that high frequencies in the tropics (such as tropical disturbance timescale of 3 to 7 days) provide energy for the maintenance of the MJO timescale. As forecast length increases so do errors in forecasts, which apply also to these energy exchanges for the high frequencies (that carry more of the errors because of larger energy within them) to the low frequencies. This is shown by Krishnamurti *et al.*[49] where they looked at a string of ECMWF medium range forecasts. They noted that a string of days 0, 1, 2 and 3 of their forecasts carried a reasonable signal of the ISO. Day 5 of forecasts had already acquired sufficient errors such that a string of days 5 of forecasts failed to show any signal of the ISO. Since both high and low frequencies are simultaneously present in these forecasts, the error growth and the contamination of the low frequencies were quite large[49]. This led to the notion that a total removal of the high frequencies at the start of a forecast experiment, $t = 0$, may be worth exploring. The initial state for these experiments contained a time mean state (averaged field covering 120 days prior to day 0), all variables time filtered from past data sets to only include the ISO timescale (20 to 60 days) and SST anomalies over the ocean are simply extrapolated from the past 120 days of the SST fields.

Conclusions

We have examined the mechanisms that explain zonal and meridional propagations of organized cloudbands on intraseasonal scales. Theories for both poleward and zonal movement of TCZ show that air–sea interaction is a major factor that modulates intraseasonal variation. We have also used a coupled ocean–atmosphere model for forecasts of intraseasonal oscillations. The results show that inclusion of sub-surface ARGO data improves the prediction of intraseasonal oscillations.

Further work is needed to understand whether the MJO/ISO is an intrinsic oceanic or atmospheric or a truly coupled mode. We have made some progress in modelling and forecasting this mode over the timescale of one month to a season. The current state of the modelling leaves many issues still unanswered.

1. Maloney, E. D. and Hartmann, D. L., The sensitivity of intraseasonal variability in the NCAR CCM3 to changes in convective parameterization. *J. Climate*, 2001, **14**, 2015–2034.
2. Randall, D., Khairoutdinov, M., Arakawa, A. and Grabowski, W., Breaking the cloud parameterization deadlock. *Bull. Am. Meteorol. Soc.*, 2003, **84**, 1547–1564.
3. Zhang, G. J. and Mu, M., Simulation of the Madden–Julian oscillation in the NCAR CCM3 using a revised Zhang–McFarlane convection parameterization scheme. *J. Climate*, 2005, **18**, 4046–4064.
4. Lau, K.-M. and Peng, P. H., Origin of low frequency (intraseasonal) oscillations in the tropical atmosphere. Part I: The basic theory. *J. Atmos. Sci.*, 1987, **44**, 950–972.
5. Nakazawa, T., Tropical super clusters within intraseasonal variations over the western Pacific. *J. Meteorol. Soc. Jpn.*, 1988, **66**, 823–839.
6. Zhang, G. J. and McFarlane, N. A., Sensitivity of climate simulations to the parameterization of cumulus convection in the Canadian Climate Centre general circulation model. *Atmos. Ocean*, 1995, **33**, 407–446.
7. Wang, B. and Xie, X., A model for the Boreal summer intraseasonal oscillation. *J. Atmos. Sci.*, 1997, **54**, 72–86.
8. Fu, X. H. and Wang, B., The Boreal-summer intraseasonal oscillations simulated in a hybrid coupled atmosphere–ocean model. *Mon. Weather Rev.*, 2004, **132**, 2628–2649.
9. Lindzen, R. S., Wave–CISK in the tropics. *J. Atmos. Sci.*, 1974, **31**, 156–179.
10. Sikka, D. R. and Gadgil, S., On the maximum cloud zone and the ITCZ over Indian longitudes during the southwest monsoon. *Mon. Weather Rev.*, 1980, **108**, 1840–1853.
11. Hoskins, B. and Wang, B., Large-scale atmospheric dynamics. In *The Asian Monsoons* (ed. Wang, B.), Springer–Praxis, Chichester, UK, 2006, pp. 357–415.
12. Waliser, D., Intraseasonal variability. In *The Asian Monsoons* (ed. Wang, B.), Springer–Praxis, Chichester, UK, 2006, pp. 203–257.
13. Charney, J. G. and Eliassen, A., On the growth of the hurricane depressions. *J. Atmos. Sci.*, 1964, **21**, 68–75.
14. Ooyama, K., A dynamic model for the study of tropical cyclone development. *Geofis. Int.*, 1964, **4**, 187–198.
15. Yamasaki, M., Large-scale disturbances in conditionally unstable atmosphere in low latitudes. *Papers Meteorol. Geophys.*, 1969, **20**, 289–336.
16. Lau, K.-M., Peng, L., Sui, C.-H. and Nakazawa, T., Dynamics of supercloud clusters, westerly wind burst, 30–60 day oscillations, and ENSO: An unified view. *J. Meteorol. Soc. Jpn.*, 1989, **67**, 205–219.
17. Sui, C. H. and Lau, K.-M., Origin of low-frequency (intraseasonal) oscillations in the tropical atmosphere. Part II: Structure and propagation of mobile wave–CISK modes and their modification by lower boundary forcings. *J. Atmos. Sci.*, 1989, **46**, 37–56.
18. Cho, H. R. and Pendelbury, D., Wave–CISK of equatorial waves and the vertical distribution of cumulus heating. *J. Atmos. Sci.*, 1997, **54**, 2429–2440.
19. Emanuel, K. A., An air–sea interaction model of intraseasonal oscillations in the tropics. *J. Atmos. Sci.*, 1987, **44**, 2324–2340.
20. Neelin, J. D., Held, I. M. and Cook, K. H., Evaporation-wind feedback and low-frequency variability in the tropical atmosphere. *J. Atmos. Sci.*, 1987, **44**, 2341–2348.
21. Brown, R. G. and Bretherton, C. S., Tropical wave instabilities: convective interaction with dynamics using the Emanuel convection parameterization. *J. Atmos. Sci.*, 1995, **50**, 2922–2939.
22. Lin, J. W. B., Neelin, J. D. and Zeng, N., Maintenance of tropical intraseasonal variability. Impact of evaporation–wind feedback and midlatitude storms. *J. Atmos. Sci.*, 2000, **57**, 2793–2823.
23. Mathew, A. J., Propagation mechanisms for the Madden–Julian oscillation. *Q. J. R. Meteorol. Soc.*, 2000, **126**, 2637–2652.
24. Maloney, E. D., An intraseasonal oscillation composite life cycle in the NCAR CCM3.6 with modified convection. *J. Climate*, 2002, **15**, 964–982.
25. Blade, I. and Hartmann, D. L., Tropical intraseasonal oscillation in a simple nonlinear model. *J. Atmos. Sci.*, 1993, **50**, 2922–2939.
26. Kemball-Cook, S. R. and Weare, B. C., The onset of convection in the Madden Julian oscillation. *J. Climate*, 2001, **14**, 780–793.
27. Krishnamurti, T. N., Chakraborti, D. R., Cubukcu, N., Stefanova, L. and Kumar, T. S. V. V., A mechanism of the Madden–Julian oscillation based on interactions in the frequency domain. *Q. J. R. Meteorol. Soc.*, 2003, **129**, 2559–2590.
28. Rajendran, K., Nanjundiah, R. S. and Srinivasan, J., The impact of surface hydrology on the simulation of tropical intraseasonal os-

cillation in NCAR (CCM2) atmospheric GCM. *J. Meteorol. Soc. Jpn.*, 2002a, **80,** 1357–1381.
29. Yasunari, T., A quasi-stationary appearance of 30 to 40 day period in the cloudiness fluctuations during the summer monsoon over India. *J. Meteorol. Soc. Jpn.*, 1980, **8**, 225–229.
30. Shanker, A. P. and Nanjundiah, R. S., Morlet wavelet analysis in space and time: study of poleward propagations of intertropical convergence zones. *Geophys. Res. Lett.*, 2004, **31**, doi: 10.1029/2003GL018150.
31. Gadgil, S., The Indian monsoon and its variability. *Annu. Rev. Earth Planet. Sci.*, 2003, **31**, 429–467.
32. Lau, K.-M and Lau, N. C., Observed structure and propagation characteristics of tropical summertime disturbances. *Mon. Weather Rev.*, 1990, **118**, 1888–1913.
33. Sengupta, D. and Ravichandran, M., Oscillation of Bay of Bengal sea surface temperature during 1998 summer monsoon. *Geophys. Res. Lett.*, 2001, **28**, 2033–2036.
34. Zheng, Y., Waliser, D. E., Stern, W. F. and Jones, C., The role of coupled sea–surface temperatures in the simulation of the tropical intraseasonal oscillation. *J. Climate*, 2004, **17**, 4109–4134.
35. Webster, P. J., Mechanisms of low-frequency variability: Surface hydrological effects. *J. Atmos. Sci.*, 1983, **32**, 427–476.
36. Nanjundiah, R. S., Srinivasan, J. and Gadgil, S., Intraseasonal variation of the Indian summer monsoon. II: Theoretical aspects. *J. Jpn. Meteorol. Soc.*, 1992, **70**, 529–550.
37. Gadgil, S. and Srinivasan, J., Low frequency variation of tropical convergence zones. *Meteorol. Atmos. Phys.*, 1990, **44**, 119–132.
38. Srinivasan, J., Gadgil, S. and Webster, P. J., Meridional propagation of large-scale monsoon convective zones. *Meteorol. Atmos. Phys.*, 1993, **52**, 15–35.
39. Rajendran, K., Nanjundiah, R. S. and Srinivasan, J., Comparison of seasonal and intraseasonal variation of tropical climate in NCAR CCM2 GCM with two different cumulus schemes. *Meteorol. Atmos. Phys.*, 2002b, **79**, 57–86.
40. Waliser, D. E., Lau, K. M. and Stern, W., Potential predictability of the MJO. *Bull. Am. Meteorol. Soc.*, 2003, DOI: 10.1175/BAMS-84-1-33.
41. Waliser, D. E. *et al.*, The experimental MJO prediction project. *Bull. Am. Meteorol. Soc.*, 2006, DOI: 10.1175/BAMS–87-4-425.
42. Xavier, P. and Goswami, B. N., A promising alternative to prediction of seasonal mean all India rainfall. *Curr. Sci.*, 2007, **93**, 195–202.
43. Krishnamurti, T. N., Chakraborty, A., Krishnamurti, R., Dewar, W. K. and Clayson, C. A., Passage of intraseasonal waves in the sub-surface oceans. *Geophys. Res. Lett.*, 2007 (submitted).
44. LaRow, T. E. and Krishnamurti, T. N., Initial conditions and ENSO prediction using a coupled ocean–atmosphere model. *Tellus*, 1998, **50A**, 76–94.
45. Krishnamurti, T. N. *et al.*, Coupled atmosphere–ocean modeling of the El Niño of 1997–98. *J. Climate*, 2000, **13**, 2428–2459.
46. Krishnamurti, T. N., Xue, J., Bedi, H. S., Ingles, K. and Oosterhof, D., Physical initialization for numerical weather prediction over the tropics. *Tellus*, 1991, **3AB**, 53–81.
47. Krishnamurti, T. N. *et al.*, Improved skill for the anomaly correlation of geopotential heights at 500 hPa. *Mon. Weather Rev.*, 2003b, **131**, 1082–1102.
48. Krishnamurti, T. N. and Subrahmanyam, D., The 30–50 day mode at 850 mb during MONEX. *J. Atmos. Sci.*, 1982, **39**, 2088–2095.
49. Krishnamurti, T. N. *et al.*, Predictability of low-frequency modes. *Meteorol. Atmos. Phys.*, 1990, **44**, 63–83.
50. Krishnamurti, T. N., One-month forecasts of wet and dry spells of the monsoon. *Mon. Weather Rev.*, 1992, **120**, 1191–1223.
51. Krishnamurti, T. N., Han, S. O. and Misra, V., Prediction of the dry and wet spell of the Australian monsoon. *Int. J. Climatol.*, 1995, **15**, 753–771.
52. Krishnamurti, T. and Chakraborty, D. R., The dynamics of phase locking. *J. Atmos. Sci.*, 2006, **62**, 2952–2964.